Available online at www.sciencedirect.com
SCIENCE DIRECT
Polymer 47 (2006) 2147–2155
polymer
www.elsevier.com/locate/polymer

Quantitative analysis of small angle neutron scattering data from montmorillonite dispersions

Helen E. Hermes *, Henrich Frielinghaus, Wim Pyckhout-Hintzen, Dieter Richter

Institut für Festkörperforschung, Research Centre Jülich, 52425 Jülich, Germany

Received 30 November 2005; received in revised form 16 January 2006; accepted 17 January 2006
Available online 7 February 2006

Abstract

A new model is presented which can describe quantitatively the small angle neutron scattering from montmorillonite-type clay dispersions and polymer-clay nanocomposites. The model is shown to be able to describe well the data from a series of dilute montmorillonite in water dispersions in which the deuterium content of the water phase is varied. The fits combined with information from other techniques suggest strongly that H–D exchange occurs in the montmorillonite-water dispersions. Deviations from Q^{-2} behaviour often observed experimentally for clay dispersions are convincingly explained by the presence of a small proportion of tactoids.

Keywords: Montmorillonite; Nanocomposite; Small angle neutron scattering

1. Introduction and background

The interactions between polymers and clays have been studied for many years [1]. Interest in this subject has exploded [2] since the development and commercialisation of nylon-montmorillonite nanocomposites by Toyota. Commercially, these materials are of interest because at low clay contents significant improvements in, for example, mechanical properties, heat distortion temperature and gas permeability may be observed. In addition, due to the nature of the dispersed clay particles, such clay-polymer nanocomposites may be processed on standard machinery and transparency may be preserved. On an academic level, these materials are of interest as 'model' high aspect ratio fillers. In the case of high clay content materials in which the polymer is completely confined on a (sub-)nanometre scale between the clay platelets, they are also systems in which the effect of extreme confinement can be studied

Sodium montmorillonites are the clays most commonly used as the basis for polymer-clay nanocomposites. They are naturally occurring expandable 'smectite' clays, or 'layered silicates' with an average chemical formula of $[Si_4Mg_{0.33}Al_{1.67}H_2O_{12}][Na]_{0.33}$. The individual clay sheets are just under 1 nm-thick and have lateral dimensions of the order of hundreds of nanometers. In the dry state these 'platelets' are present as stacks known as 'tactoids'. When interactions with the clay are favourable, solvent or polymer can intercalate between the platelets forming a 'sandwich' structure. Intercalation increases the interlayer distance between the platelets. This can be measured for example, by X-ray diffraction. It is possible for the interlayer distance to increase to such an extent that the platelets become 'exfoliated'. Fig. 1 illustrates schematically the stacked and exfoliated structures. In reality, a single sample may contain both tactoids and individual platelets.

Neutron scattering has been used for some time to investigate clay dispersions [3]. The interaction of polymers with such dispersions has also been widely examined using this technique [4]. By (partial) deuteration of, for example, the solvent, the contrast between the system components can be varied. As a result neutron scattering experiments can reveal information not available from X-ray scattering which has been used more extensively. In comparison with techniques such as infra-red or nuclear magnetic spectroscopy which study materials on the atomic level, neutron scattering looks at a larger scale and can be used to study, for example, the effect of clay on the conformation of polymer chains

Over the last several years Ho, Hanley, Glinka and co-workers have presented a large volume of SANS data from montmorillonite and organoclay dispersions [5]. For the

* Corresponding author. Address: Physik der weichen Materie, IPkM, Heinrich-Heine-Universität Düsseldorf, 40225 Düsseldorf, Germany. Tel.: +49 (0) 211 81 14812; fax: +49 (0) 211 81 14850.
E-mail address: helen.hermes@uni-duesseldorf.de (H.E. Hermes).

0032-3861/$ - see front matter © 2006 Elsevier Ltd. All rights reserved.
doi:10.1016/j.polymer.2006.01.059

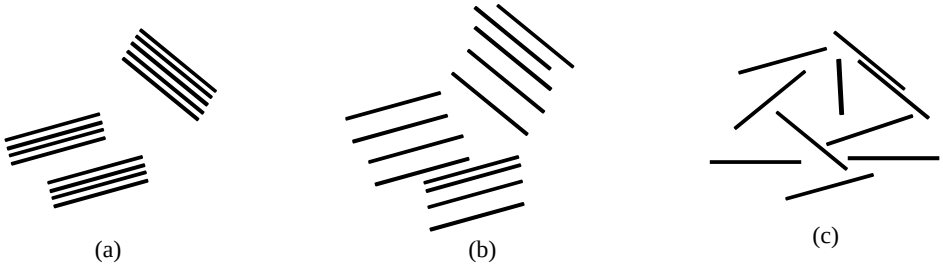

Fig. 1. Schematic illustration of (a) tactoids, (b) intercalated tactoids and (c) exfoliated clay platelets.

organoclays (clays such as montmorillonite in which the inorganic ion has been replaced by an organophilic compound, usually a surfactant) they have investigated in detail the effect of solvent solubility parameters on the degree of distribution of the clay. To quantitatively describe the scattering data they have developed a core-layer model. They assume that the next neighbour distance in a stack of platelets obeys a Gaussian distribution. The fits shown are for data from samples with good contrast and are of good quality. In agreement with previous studies, they find that montmorillonite in water is dispersed as individual platelets. For the organoclay dispersions they find that the degree of dispersion depends on the solubility parameter of the solvent

This paper introduces a new fitting model which has been developed to quantitatively describe the scattering data from montmorillonite platelets distributed as individual platelets and/ or tactoids in a matrix which can be either a polymer or a solvent. As described in more detail in the next section, it differs from previous models in that it concentrates on the larger scale, i.e. low Q-range scattering data, which is related to the way in which the platelets are distributed within the matrix, rather than focussing on the internal structure of the tactoids. This novel approach reveals information useful for explaining, for example, the mechanical properties of clay nanocomposites. The accuracy of the model is demonstrated on the basis of SANS data from a series of dilute dispersions of montmorillonite in water. Although the model is also capable of describing organically modified clay systems, this initial work concentrates on systems based on unmodified montmorillonite. This reduces the number of components in the system and thus the ambiguity of the fits

2. Proposed scattering model

The formation of intercalated tactoids is a multi-scale phenomenon. On short length scales, a sandwich structure of clay platelets and polymer or solvent is present. The thickness of the intercalated material is not necessarily constant, i.e. the internal structure of a tactoid is not strictly regular. Such short range structures are frequently observed and described as Bragg-peaks in the intermediate Q-range of X-ray scattering experiments. Models published previously have described this internal structure and the particle as a whole. By contrast, whole tactoids are observed in the Q-range of a typical SANS experiment such as described in this paper. Thus, our model does not need to describe the internal structure, and, a completely regular structure of the stacks is assumed. In order to describe the scattering pattern from a many-particle system the interactions between these must generally be included. Correlations between the large tactoids are difficult to treat due to the large aspect ratio (structure factors for spherical particles are much more simple). However, in the dispersions discussed in this paper, the concentration is low enough to neglect large scale correlations.

In our SANS model we focus on the appearance of the tactoid as a whole particle. We successfully describe the statistics of the platelet number as simply as possible. The internal structure is assumed to be regular. The previous model by Hanley [5] assumed a Gaussian distribution of the platelet distance. These distortions of the first kind affect the Bragg peak width. The distribution of the platelet number used is important to describe SANS scattering data but it is not described explicitly by Hanley and co-workers. A more general model of the internal structure which allows for these distortions of the second kind was presented by Vaia and co-workers [6]. However, this model failed to describe the scattered intensity over the SANS Q-range. As shown below, our refined model of the platelet number statistics does ensure a good description in the SANS Q-range. The simplified assumption of a regular internal structure leads to analytical expressions of the structure factor S_{platelet}. A combination of the Vaia model with our description of the platelet number statistics could lead to a model describing the SANS Q-range and the Bragg peaks observed at higher Q-values. However, this combination would involve a numerical summation, which would increase computational times significantly. In this paper this refinement is not discussed further as our data do not cover this Q-range.

In detail, the simple model we propose starts with a single clay platelet with half of the polymer/solvent layer on either side of the elementary particle. This is described by the form factor F_{platelet}. The formation of the whole tactoid is described by the structure factor S_{platelet}. The detailed derivation of expressions for these factors is given in the Appendix. The whole tactoid is orientationally averaged, since no direction is preferred. Thus, substituting in our expressions for the structure and form factor yields the following expression for scattering from clay systems

$$\frac{d\Sigma}{d\Omega}(Q) = \phi(1-\phi)\int S_{\text{platelet}}(Q_z)F_{\text{platelet}}(Q_{xy},Q_z)\sin(\beta)\,d\beta \quad (1)$$

The components of the scattering vector are given by the angle β, namely $Q_z = |Q|\cos\beta$ and $Q_{xy} = |Q|\sin\beta$. The tactoid fraction ϕ appears in the prefactor as for concentrated systems. The form factor F_{platelet} factorizes by two amplitudes, which describe the in-plane structure of a disc and the platelet structure in the normal (z)-direction and is given by:

$$F_{\text{platelet}}(Q) = \frac{|A_{\text{disc}}(Q_{xy})A_z(Q_z)|^2}{V_{\text{platelet}}} \quad (2)$$

Normalisation by the single platelet volume V_{platelet} ensures the form factor is proportional to the actual volume.

The structure factor takes into account the statistics of the tactoid formation and is given by:

$$S_{\text{platelet}}(Q_z) = \left\langle \left(\frac{\sin\left(\frac{1}{2}d_zQ_zk\right)}{\sin\left(\frac{1}{2}d_zQ_z\right)} \right)^2 \right\rangle_k / \langle k\rangle_k \quad (3)$$

The inner bracket describes a structure factor with a given number of platelets k. Normalization by the average number of platelets yields the structure factor describing the mass average of the tactoids. In the low Q-limit the structure factor is $S_{\text{platelet}}(Q_z) = \langle k^2\rangle/\langle k\rangle$.

In this model, the statistics assumed for the platelet distribution are the sum of a Poisson distribution and a box (flat homogenous) distribution. The parameters are: the mean platelet number λ of the Poisson distribution, the maximum platelet number N of the box distribution, and a weight parameter α, which describes the dominance of the Poisson distribution. This assumption results in a small number of parameters and seems to agree with published microscopy results [7].

The model can be used to illustrate the effect of different degrees of platelet dispersion on the scattering pattern. For each simulation the scattering length densities of the clay and solvent, the dimensions of the individual clay platelets and the clay content were kept constant. The effect of increasing the proportion of platelets present as tactoids is illustrated in Fig. 2. When all platelets are present as individual platelets (i.e. $\alpha = 0$), the slope of the data in a log–log plot is seen to be -2.0 as expected for non-interacting thin discs. If 1% of the platelets are present as tactoids containing an average of 7 platelets, the shape of the scattering curve changes minimally and the slope decreases to approximately -2.2. Experimentally, slopes of this order are often observed for clay dispersions. Increasing the proportion of tactoids to 10% can be seen to have a more significant effect on the scattering pattern. Careful observation reveals two different slopes. This is because a sufficient proportion of discs no longer meet the thin disc criterion such that a Q^{-4} 'Porod-law' component resulting from the surfaces of the particles starts to become visible. This component is clearer for the highest intensity curve which is a simulation which assumes that all platelets are present as tactoids containing on average 7 platelets. Here both the Q^{-2} component resulting from the platelets making up the tactoids and the Q^{-4} component describing the surface scattering from the tactoids are clearly visible. The change in slope occurs at a Q-value approximately equal to the inverse of the average thickness of the tactoid. This is clearly illustrated in Fig. 3 which illustrates the effect on the scattering pattern of average number of platelets per tactoid if all the clay is present in this form. These results illustrate that the experimentally observed deviations from a Q^{-2} slope in scattering data from clay dispersions are due to the presence of a small proportion of tactoids, i.e. non-exfoliated platelets, such that a Q^{-4} surface scattering component is superimposed on the Q^{-2} scattering from the non-interacting thin discs.

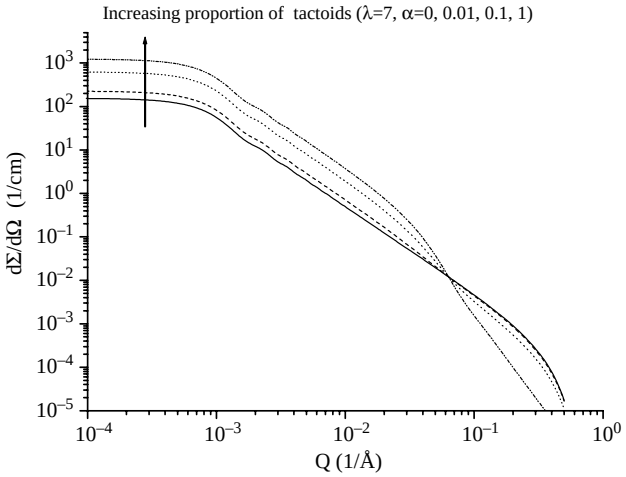

Fig. 2. Simulation results illustrating the effect of the presence of tactoids on the scattering pattern. Parameters used: $\rho_{\text{clay}} = 3.9\times10^{10}\,\text{cm}^{-2}$, $\rho_{\text{surr}} = 5.34\times10^{10}\,\text{cm}^{-2}$ (85% D_2O), $d_{\text{clay}} = 9.5$ Å, $D = 5000$ Å, $\lambda = 7$, $N = 1$, $\alpha = 0$, 0.01, 0.1, or 1, $\phi = 0.004$.

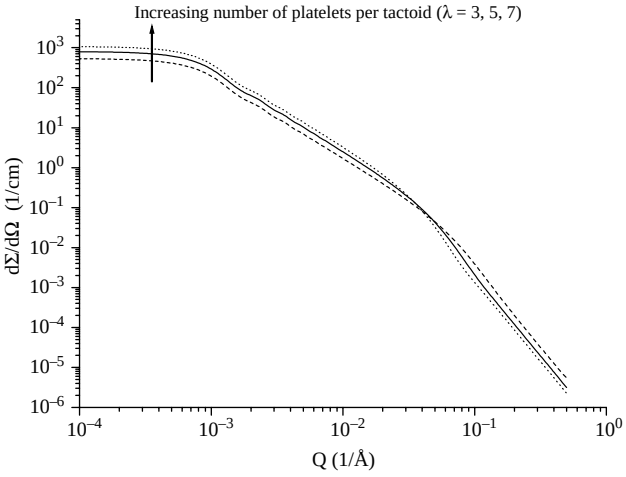

Fig. 3. Simulated results illustrating the effect of number of platelets per tactoid on the scattering pattern. Parameters used $\rho_{\text{clay}} = 4\times10^{10}\,\text{cm}^{-2}$, $\rho_{\text{surr}} = 5.34\times10^{10}\,\text{cm}^{-2}$ (85% D_2O), $d_{\text{clay}} = 9.5$ Å, $D = 5000$ Å, $\lambda = 3$, 5, or 7, $\alpha = 1$, $\phi = 0.004$.

3. Experimental methods

3.1. Materials

The sodium montmorillonite used, Nanofil 757, was generously donated by Süd-Chemie, Moosberg, Germany. According to the producer it is a highly pure sodium montmorillonite with a density of approximately 2.6 g/cm^3, a cationic exchange capacity (CEC) of 80 mVal/100 g, and a particle size of approximately 100–500 by 1 nm when fully dispersed.

3.2. Sample preparation

To ensure that the montmorillonite in water dispersions remained stable, i.e. did not settle, the montmorillonite was fractionated prior to use using centrifugation in two stages. For this an approximately 1 wt% dispersion of the clay in Millipore water was prepared a day before centrifugation. To aid exfoliation of the clay the dispersion was treated in an ultrasound bath. After fractionation the water was removed by freeze drying to a constant weight. The montmorillonite was then placed in a vacuum oven at room temperature.

The 1 wt% dispersions for the scattering experiments were prepared directly using the required H–D composition of the water phase and a known quantity of clay. Millipore water and high purity D_2O were used. To ensure maximum dispersion, i.e. exfoliation, the dispersions were placed in an ultrasound bath. All dispersions were treated in an identical manner and were optically clear. They were prepared 3 days prior to the SANS experiments.

3.3. Small angle neutron scattering (SANS)

The SANS experiments were performed on the KWS1 and KWS2 instruments at the Forschungszentrum in Jülich. These instruments have been described elsewhere [8]. The dispersions were placed in 1mm gap quartz cells. The SANS measurements were performed at room temperature. By using the neutron wavelength $\lambda = 7$ Å and sample-detector distances of 2 and 8 m, scattering data were collected over the Q-ranges 0.0045–0.125 Å^{-1}. The scattering patterns were isotropic. The data was azimuthally averaged before being corrected for sample transmission, empty cell, etc. and placed on an absolute scale using standard procedures

3.4. X-ray scattering

X-ray scattering data were collected using a Bruker AXS D8 X-ray reflectometer [9] and a wavelength of 1.54 Å. The dispersions were placed in an open trough. During these measurements the water gradually evaporated such that several repeat measurements were performed as a function of concentration. These experiments were performed using the dispersions which had been prepared for the SANS experiments. The dispersions had been stored in sealed glass vials in the dark at room temperature. They did not exhibit any signs of settling or degradation and were optically identical. The data were interpreted in terms of the peak position. In addition, the average number of platelets per tactoid was estimated using the Scherrer equation [10]. For these calculations, instrumental broadening was neglected and a value for the Scherrer constant of 0.9 was used such that the equation becomes:

$$t = \frac{0.9\lambda}{B\cos\theta} \tag{4}$$

where t is the average thickness of the tactoid, λ is the wavelength of the X-rays, B is the width of the observed diffraction line at its half-intensity maximum and θ is the peak position of the diffraction line. B and θ must be given in radians. As the thickness of an individual platelet is known, the average number of platelets per tactoid can be estimated from t.

4. Results and discussion

Two randomly chosen montmorillonite in water dispersions which had been previously investigated using SANS were investigated using X-ray scattering as a function of time, i.e. concentration. The dispersions had been prepared concurrently and were optically identical. Fig. 4 illustrates typical data obtained. The broad halo at $Q > 1$ Å^{-1} can be correlated with the structure of water. Changes in the water halo were observed for both dispersions as a function of concentration. This may indicate a change in the structure of the water due to increasing interactions with the clay. As this was not of direct interest in this work, the effect was not investigated further. Pertinent to this work is the distribution of the clay platelets. If the clay platelets are fully exfoliated and randomly distributed, no peak will be observed in the WAXS data. This was initially the case for one dispersion. As illustrated in Fig. 4, the other dispersion exhibited a peak just below $Q = 0.5$ Å^{-1}. The position and sharpness of the peak indicate that in this dispersion tactoids with an interlayer distance of 15.7 Å and an average number of platelets per tactoid of approximately 7 are present (Scherrer equation). This interlayer distance is similar to that previously

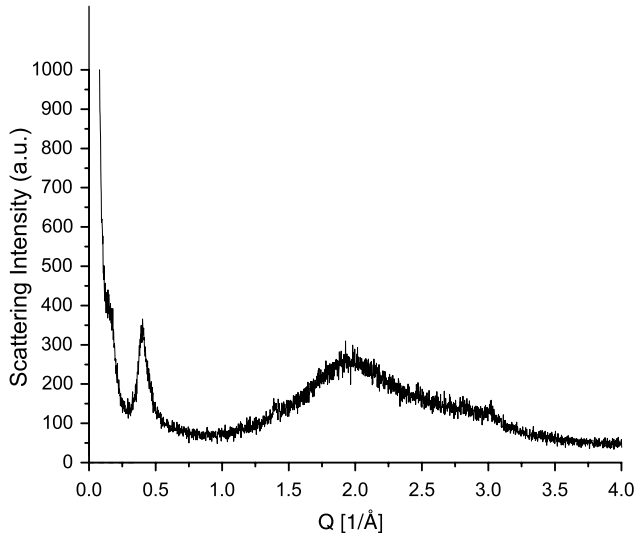

Fig. 4. WAXS data from a 1 wt% MMT in water (85 vol.% D_2O) dispersion.

reported for the second hydration level in which the sodium ion is surrounded by 12 water molecules [11]. As the concentration of the dispersions increased due to evaporation, the peak became visible in the data from both dispersions. Its intensity subsequently increased indicating an increase in the average number of platelets per tactoid with concentration. The position of the peak did not change. For the detailed fitting of SANS data discussed below, these X-ray scattering results thus yield following information:

1. Tactoids may be present in optically clear dispersions
2. The platelet distribution in optically identical and concurrently prepared dispersions may vary
3. The tactoids exhibit an average interlayer distance of approximately 15.7 Å.

The complete series of nine 1 wt% montmorillonite in water dispersions in which the H–D composition of the water phase was varied systematically from 0 to 85% D_2O was investigated using SANS. Fig. 5 illustrates typical data obtained. One aim of these experiments was to obtain an experimental value for the scattering length density of the montmorillonite. Generally, the scattering intensity can be described as [12]: $d\Sigma/d\Omega(Q) = \phi(1-\phi)V(\Delta\rho)^2 P_{tactoid}(Q)S_{tactoid}(Q)$, where ϕ is the volume fraction of clay, V is the average volume of a scattering particle, i.e. of a tactoid, $(\Delta\rho)^2$ is the contrast resulting from the difference in scattering length density between the particles and matrix, $P_{tactoid}(Q)$ is the form factor, which describes the shape of the particles and $S_{tactoid}(Q)$ is the structure factor which describes the interactions between the particles. As already discussed, the structure factor of the tactoids is safely neglected. Hence, if the concentration and nature (which yields $P_{tactoid}(Q)$) of the particles in a dispersion are kept constant, the observed scattering intensity is proportional only to the square of the contrast between the particle and the matrix, in this case solvent [13]. When the scattering length density of the particles and the solvent are identical, the scattering intensity will be theoretically zero. Practically, due to inhomogeneities in the particles the minimum value is often not zero. Nevertheless, the average scattering length density of particles can be found by plotting the square root of the scattering intensity at a particular small Q-value against the scattering length density of the solvent. Fig. 6 illustrates such a plot for the dispersions measured. From this the average scattering length density of the montmorillonite appears to be slightly higher than 4×10^{10} cm^{-2} which is somewhat higher than the calculated values of 3.85×10^{10} cm^{-2} obtained if a density of 2.66 g cm^{-3} is assumed [5] or 3.74×10^{10} cm^{-2} for a density of 2.6 g cm^{-3}. This deviation may be explained in terms of compositional variations and impurities in a natural product such as sodium montmorillonite. However, as will be shown below, the true reason is that the scattering length density of the clay actually varies with solvent composition due to H–D exchange

The data from all dispersions were fit using our model described in detail above. Figs. 7 and 8 illustrate typical data (background has in this case not been removed) and fits together with the obtained platelet distributions. For the dispersions with good contrast, it was possible to fit the data simply assuming that clay platelets with a constant (calculated or experimentally measured) scattering length density were present as a mixture of exfoliated platelets and tactoids in a solvent of constant scattering length density. This was not the case for the low contrast samples so that the two alternative models discussed below were considered. When the scattering length density of the clay was assumed to be constant, fits using both 3.9×10^{10} and 4.0×10^{10} cm^{-2} were performed. Table 1 summarises which model was capable of fitting the data from each dispersion.

4.1. Bound water layer

The existence on clay surfaces of a water layer with a structure different to that in the bulk was suggested many years ago [14]. NMR, X-ray diffraction and Monte Carlo simulations have confirmed this [15] and suggest that the bound water layer is more ‘solid’ than bulk water. By contrast, small angle X-ray data have been interpreted to suggest an ‘electron inhomogeneity’ at the montmorillonite interface one interpretation of

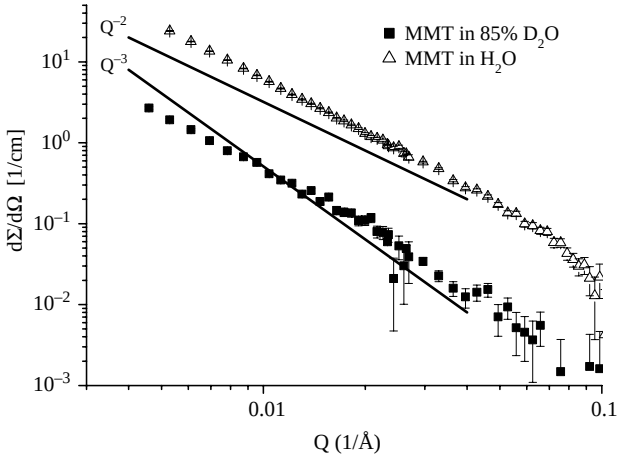

Fig. 5. Typical SANS data for 1 wt% montmorillonite in water dispersions.

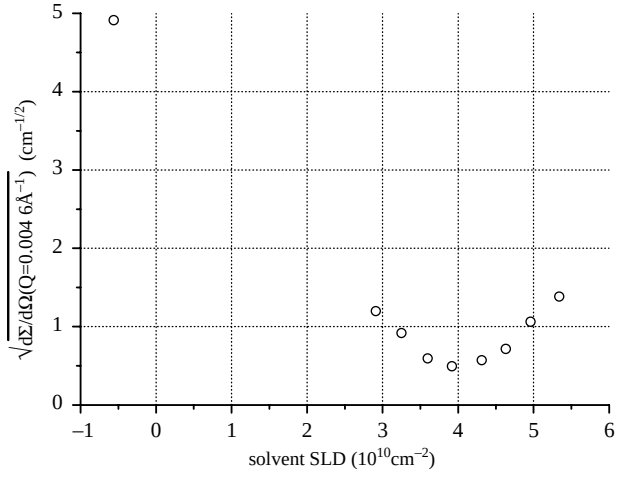

Fig. 6. Experimental contrast variation plot for 1 wt% MMT in water.

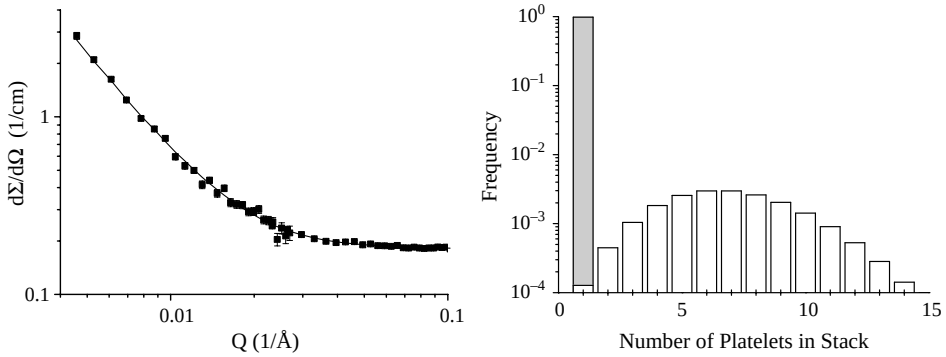

Fig. 7. (a) typical fit (line) to data (symbols) from MMT in 85% D2O dispersion (b) illustration of platelet distribution used in fit Parameters used: $\phi=0.004$, $\rho_{clay}=4.25\times10^{10}$ cm^{-2}, $\rho_{inter}=\rho_{surr}=5.34\times10^{10}$ cm^{-2}, $d_{clay}=9.5$ Å, $d_{inter}=3.1$ Å, $D=5000$ Å, $\lambda=7$, $N=1$, $\alpha=0.02$.

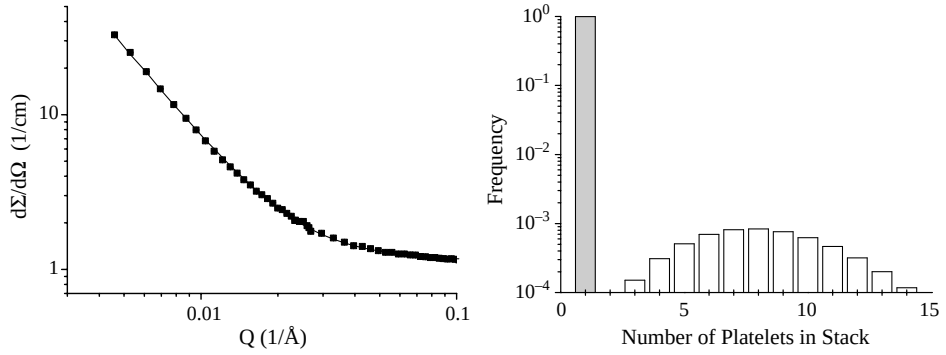

Fig. 8. (a) typical fit (line) to data (symbols) from MMT in 100% H_2O dispersion (b) illustration of platelet distribution used in fit. Parameters used: $\phi=0.004$, $\rho_{clay}=3.90\times10^{10}$ cm^{-2}, ρinter$=\rho_{surr}=-0.56\times10^{10}$ cm^{-2}, $d_{clay}=9.5$ Å, $d_{inter}=3.1$ Å, $D=5000$ Å, $\lambda=7$, $N=1$, $\alpha=0.006$.

which may be that the density of the adsorbed water is lower than that of 'free' water [16]

The SANS data from the nine dispersions investigated in this work were fit using both a lower and a higher density water layer attached to the montmorillonite platelets. The thickness of the layer was generally fixed at 3.1 Å ([15.7−9.5]/2). The lower density layer model was not successful at describing the scattering from more than half the dispersions and was thus discarded. By contrast all the data could be fit by assuming that the water layers adjacent to the clay platelets have a density higher than the bulk density of water. In almost all cases a density 10% higher than the bulk water value could be

Table 1
Summary of quality of fits to data from montmorillonite in water dispersions for different physical models

Sample number	1	2	3	4	5	6	7	8	9
% D_2O in water phase	85	80	75	70	65	60	55	50	0
SLD of water phase (10^{10} cm^{-2})	5.340	4.958	4.632	4.313	3.917	3.598	3.251	2.911	−0.56
Fitting results									
Simple model	(✓)	✓	(✓)	✓	×	✓	✓	✓	✓
Bound water: density lower than in bulk	×	×	×	(✓)	✓	×	✓	✓	✓
Bound water: density higher than in bulk	✓	✓	✓	✓*	✓	✓	✓	✓	✓
H–D exchange	✓	✓	✓	✓	✓	✓	✓	✓	✓

✓: data could be fit successfully using this model. (✓): data could be fit using this model, but the quality of the fit was poor. ×:data could not be fit using this model.
*A different density was required for this sample (see text for details).

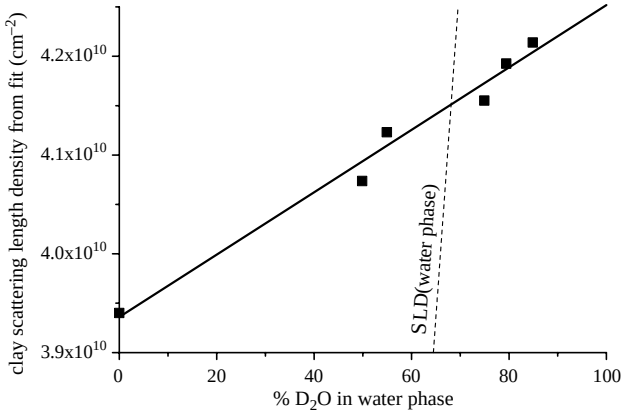

Fig. 9. Clay scattering length density obtained from fits if allow this to vary. Line: SLD(clay)(cm^{-2})$=0.316\times10^{8}$ (%D_2O in water phase)$+3.94\times10^{10}$. Dashed line calculated from D_2O content.

assumed. For one dispersion the density could only be increased by approximately 5%.

4.2. H–D exchange between the solvent and the clay such that the clay SLD changes

The possibility that H–D exchange between deuterated water and clay may occur has been discussed previously in the interpretation of neutron scattering results: Nelson and Cosgrove report a higher than expected value for the scattering length density of laponite determined experimentally using a contrast variation plot [4] whilst Smalley and co-workers discuss 'extra' peaks in a diffraction pattern of vermiculite in terms of H–D exchange [17] (laponite and vermiculite are clays with structures similar to montmorillonite). A brief survey of the literature reveals that the exchange between heavy water and montmorillonite and other clay minerals has been investigated for many years [18]. Despite this, results published for montmorillonite at ambient conditions range from rapid and almost complete exchange [19] to minimal exchange [20]. This difference may be a result of the different ways in which the D_2O and clay were contacted and/or subsequent exchange with atmospheric moisture

The SANS data for all nine dispersions were fit allowing both the scattering length density of the clay and the platelet distribution to vary. To some extent variations in these parameters have similar effects on the scattering pattern in the *Q*-range investigated. These subtle changes can be discussed in the context of trends of the whole series. The fitting results can be summarised as follows:

a. The interlayer spacing used has no significant effect on the scattering pattern in the SANS *Q*-range investigated. We therefore, used the WAXS result to fix the parameter.
b. It is not possible to fit the data assuming that the relative amounts of hydrogen and deuterium in the clay are the same as in the water phase. The water phase must contain a higher proportion of deuterium. This agrees with previous reports [21] and is presumably related to the accessibility of the hydrogen in the clay
c. Allowing the scattering length density and the platelet distribution of the clay to be fit freely yielded the values for the clay scattering length density plotted in Fig. 9. This plot does not include values for the low contrast dispersions (60, 65, 70% D_2O in the water phase) because for these dispersions allowing both variables to be fit simultaneously resulted in unreasonable fits. However, data from these dispersions could be fit using the clay scattering length density calculated using the relationship described by straight line fit illustrated in Fig. 9 and allowing only the platelet distribution to vary.
d. The distribution of the platelets was found to vary randomly from one dispersion to the next. The majority of dispersions were found to contain a high proportion of individual platelets, in some cases 100%. Generally, the number of platelets per tactoid was found to be around 7 in agreement with the X-ray scattering results.

As illustrated above, although the simple physical model of platelets distributed in the water phase can be excluded, both the bound water layer and H–D exchange models can be used to fit the data. However, the effect of these different physical models on a contrast variation plot is different. Fig. 10 is a simplified contrast variation plot. (SLD(clay)-SLD(water phase))^2, which determines the intensity of the scattering as described above if all other factors are constant, is plot as a function of the solvent scattering length density. Careful observation of the values reveals that the bound layer model does not affect the position of the minimum merely the sharpness of the curve. By contrast, assuming H–D exchange occurs according to the relationship found in Fig. 9 shifts the minimum in the contrast variation plot to a position similar to that found experimentally. Thus, combining this result with the model fits to the data strongly suggests that montmorillonite

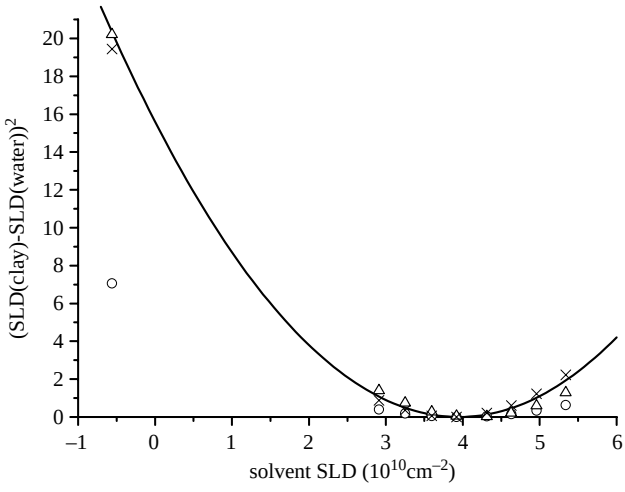

Fig. 10. Calculated contrast variation plot. The parabola illustrates the theoretical expectation. Thus the bound water layer model can be excluded. Symbols: $\times\rho_{clay}=3.85\times10^{10}$, ○: $\rho_{clay}=3.85\times10^{10}$ plus bound water layer, △: ρ_{clay} changes due to H–D exchange according to formula.

in water dispersions undergo H–D exchange with the water phase

5. Conclusions and outlook

It has been illustrated that the relatively simple new model presented can successfully describe SANS data over a wide Q-range from dilute montmorillonite in water dispersions. By fitting the data from a series of solutions with various contrast it has been shown that the montmorillonite dispersions cannot simply be depicted as platelets with constant scattering length density dispersed in the water phase. Although a bound water layer model was successful at describing the data it was shown that H–D exchange between the water phase and the clay occurs such that the scattering length density of the clay varies with the deuterium content of the water phase. In addition, the fits illustrated that the relative amounts of tactoids and exfoliated platelets in optically clear and concurrently prepared dispersions may vary. It is the presence of these tactoids which results in deviations from the Q^{-2} scattering behaviour expected from isolated thin discs. Application of the model presented to describe the neutron scattering data from polymer-clay nanocomposites is currently on-going. It has been found that the clay dispersion in these composites can again be described as a Poisson distribution coexisting with a flat unstructured (box) distribution [22]. Similar distributions have been observed directly by the interpretation of electron microscopy micrographs [7]. The model presented is sensitive not only to the SANS regime but also to the USANS regime which can be used to look at longer length scales [23]. In this paper, the lower Q-range limit yielded a lower limit of the parameter N. It is hoped that in the near future, USANS experiments will yield a more precise value for this parameter

Acknowledgements

We wish to thank Thomas Engelhardt, Süd-Chemie, Germany for donating the montmorillonite used in these experiments and for useful discussions. Ulrich Rücker is also thanked for his assistance with the X-ray scattering measurements. The neutron scattering experiments were all performed at the Research Centre Jülich, Germany.

Appendix A. Derivation of the form and structure factors used

The *form factor* of a single platelet, F_{platelet}, is given by the product of two amplitudes, which describe the structures in the plane and in the normal direction. The in-plane structure can be described as a spherical disk with diameter D

$$A_{\text{disc}}(Q_{xy}) = 2\frac{J_1\left(\frac{1}{2}\ \text{DQ}_{xy}\right)}{\left(\frac{1}{2}\right)\ \text{DQ}_{xy}}$$

where J_1 is the Bessel-function of the first kind. It should be noted that due to the lateral size of the clay particles, the shape is not observed in the experimental SANS range. Hence, the particle shape assumed is unimportant.

The structure in z-direction is given by the clay as the central particle and the intercalating material. The respective amplitudes have to be simply added:

$$A_z(Q_z) = A_{\text{clay}}(Q_z) + A_{\text{inter}}(Q_z)$$

The amplitude of a limited, one-dimensional particle then becomes:

$$A_{\text{clay}}(Q_z) = (\rho_{\text{clay}} - \rho_{\text{surr}}) \cdot V_{\text{clay}} \cdot \frac{\sin\left(\frac{1}{2}\ d_{\text{clay}}Q_z\right)}{\frac{1}{2}\ d_{\text{clay}}Q_z}$$

Here, the contrast between the clay and the surrounding is described by the scattering length density difference $\rho_{\text{clay}} - \rho_{\text{surr}}$. The volume of the clay particle is given by the thickness and the area of the disc-like particle $V_{\text{clay}} = d_{\text{clay}} \cdot \frac{\pi}{4} \cdot D^2$. Two layers of intercalating material are situated at a distance $\frac{1}{2}(d_{\text{clay}} + d_{\text{inter}})$ such that:

$$A_{\text{inter}}(Q_z) = (\rho_{\text{inter}} - \rho_{\text{surr}})V_{\text{inter}}2\cos\left(\frac{1}{2}(d_{\text{clay}} + d_{\text{inter}})Q_z\right) \times \frac{\sin\left(\frac{1}{2}d_{\text{inter}}Q_z\right)}{\frac{1}{2}d_{\text{inter}}Q_z}$$

The volume of one intercalating layer fraction is given by $V_{\text{inter}} = d_{\text{inter}} \cdot \frac{\pi}{4} \cdot D^2$. It should be stressed that such a layer fraction has half the thickness of the whole intercalating material. The full thickness of the polymer/solvent is $2d_{\text{inter}}$

The actual notation involves the contrasts and volumes for the amplitudes describing the structures in normal (z)-direction. This is due to the notation of the amplitudes of the clay and the intercalating material. Overall, the one-dimensional properties are combined with volume properties (contrast and volumes) and finally meet the area properties in the expression of the form-factor (Eq. 2).

The *structure factor* of the platelets depends on the statistics of the platelet number (Eq. 3). Two different distributions are assumed, namely a Poisson distribution and a homogenous, flat 'box' distribution. The combined structure factor reads:

$$S_{\text{platelet}}(Q_z, \lambda, N, \alpha) = (\alpha S_{\text{poisson}}(Q_z, \lambda) + (1-\alpha)S_{\text{flat}}(Q_z, N))/ \times \left(\alpha\lambda + (1-\alpha)\frac{1}{2}(N+1)\right)$$

The weight parameter α switches between the Poisson distribution ($\alpha = 1$) and the box distribution ($\alpha = 0$). The mean platelet number of the Poisson distribution is given by λ, and the maximum platelet number of the box distribution is given by N. The summation over the individual tactoids can be performed analytically. The solution for the Poisson distribution reads:

$$S_{\text{poisson}}(Q_z, \lambda) = \frac{1}{2}[1 - \cos(\lambda \sin(d_zQ_z))e^{\lambda(\cos(d_zQ_z)-1)}]/ \times \sin^2\left(\frac{1}{2}d_zQ_z\right)$$

The solution for the box distribution reads:

$$S_{\mathrm{flat}}(Q_z, N) = \frac{1}{2} \frac{\left(\frac{\sin\left(d_z Q_z \left(N+\frac{1}{2}\right)\right)}{\sin\left(\frac{1}{2} d_z Q_z\right)} - 1 \right)}{\sin^2\left(\frac{1}{2} d_z Q_z\right)}$$

The total platelet thickness is $d_z = d_{\mathrm{clay}} + 2d_{\mathrm{inter}}$. It should be noted that this structure factor assumes a regular internal structure. Only in this case are analytical expressions available. A combination of distortions of the first or second kind with these statistics is possible numerically but results in slower computation.

References

[1] Theng BKG. Formation and properties of clay-polymer complexes. Amsterdam: Elsevier; 1979.

[2] A selection of recent books and reviews includes: Pinnavaia TJ, Beal GW, editors. Polymer-clay nanocomposites. Chichester: Wiley; 2000. Utracki LA. Clay-containing polymeric nanocomposites. Shrewsbury: Rapra Technology Ltd; 2004. Alexandre M, Dubois P. Mater Sci Eng. 2000;28:1–63. Giannelis EP, Krishnamoorti R, Manias E. Adv. Polym. Sci. 1999;138:107–47.

[3] Some early examples include: Cebula DJ, Thomas RK, White JW. J.C.S. Farady I 1980;76:314–21. Burchill S, Hall PL, et al. Clay Miner 1983;18:373–97.

[4] see for example: Nelson A, Cosgrove T. Langmuir 2004;20:2298–304.

[5] see for example: Ho DL, Briber RM, Glinka CJ. Chem Mater 2001;13: 1923–31. Hanley HJM, Muzny CD, Ho DL, Glinka CJ. Langmuir 2003; 19:5575–80.

[6] Vaia RA, Liu W, Koerner H. J Pol Sci B 2003;41:3214.

[7] Yoonessi M, Toghiani H, Daulton TL, Lin J-S, Pittmann Jr. CU. Macromolecules 2005;38:818–31.

[8] http://www.fz-juelich.de/iff/wns_kws2/ and http://www.fz-juelich.de/iff/pics_pdfs/wns/exp_kws1-2.pdf and Schwahn D, Meier G, Springer TJ. Appl Cryst 1991;24:568–70.

[9] http://www.bruker-axs.de/

[10] Cullity BD. Elements of X-ray diffraction. 2nd ed. Reading, MA: Addison-Wesley; 1978 p. 101. Jenkins R, Snyder RL. Introduction to X-ray powder diffractometry. New York: Wiley; 1996 p. 90. Krawitz AD. Introduction to diffraction in materials science and engineering. New York: Wiley; 2001 p. 165.

[11] Jasmund K, Lagaly G. Tonminerale und Tone: Struktur. Eigenschaften, Anwendungen und Einsatz in Industrie und Umwelt. Darmstadt: Steinkopff; 1993 p. 105.

[12] King SM. In: Pethrick SM, Dawkins JV, editors. Modern techniques for polymer characterisation. New York: Wiley; 1999.

[13] Roe RJ. Methods of X-ray and neutron scattering in polymer science. Oxford: Oxford University Press; 2000. 230ff.

[14] Norrish K, Rausell-Colom JA. Clays Clay Miner 1963;12:123–49.

[15] Grandjean J. Encyclopedia of surface and colloid science. New York: Marcel Dekker; 2002 p. 3700–3712. Park S-H, Sposito GJ. Phys. Chem. B. 2000;104:4642–8.

[16] Shang C, Rice JA, Lin J-S. Clays Clay Miner 2001;49:277–85.

[17] Williams GD, Soper AK, Skipper NT, Smalley MV. J Phys Chem B 1998; 102:8945–9.

[18] see for example: Faucher JA, Thomas HC. J Phys Chem 1955;59:189–91.

[19] Garrone, E. Personal communication.Bodoardo S, Figueras F, Garrone E. J Catal 1994;147:223–30.

[20] Bukka K, Miller JD, Shabtai J. Clays Clay Miner 1992;40:92–102.

[21] O'Neil JR, Kharaka YK. Geochim Cosmochim Acta 1976;40:241–6.

[22] Hermes HE, Frielinghaus H, Pyckhout-Hintzen W, Richter D. In preparation.

[23] Radulescu A, Mathers RT, Coates GW, Richter D, Fetters LJ. Macromolecules 2004;37:6962–71.